

Supporting Information

S1: FTIR spectrum of MPB NPs

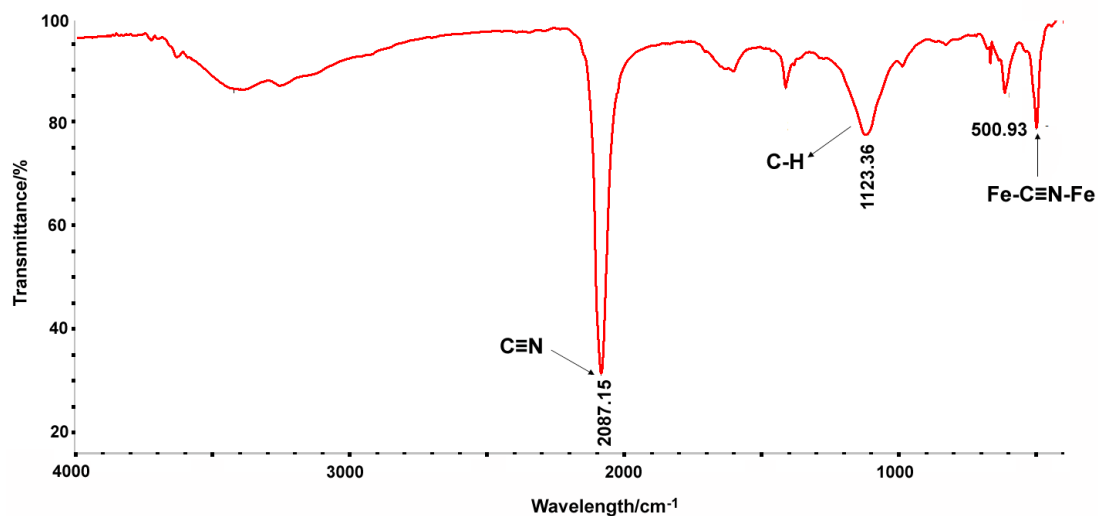


Figure S1. FTIR spectrum of MPB NPs.

S2: The particle size distribution of MPB NPs

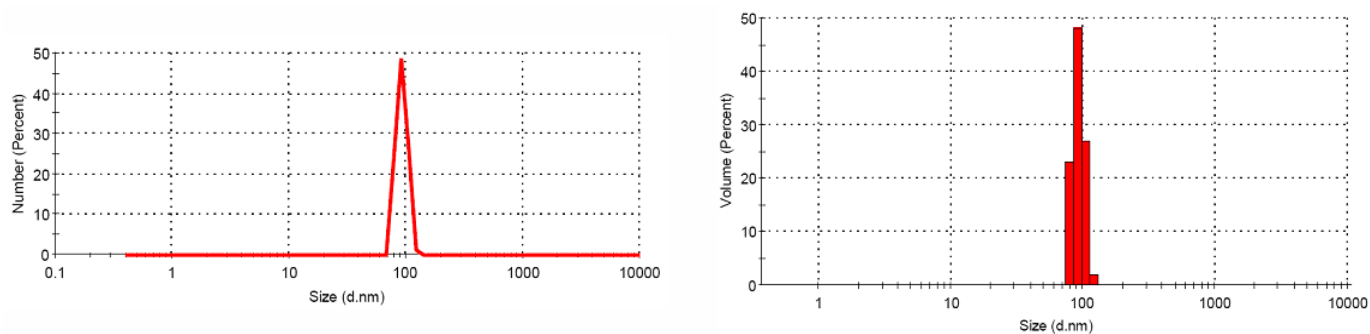


Figure S2. The DLS measurement results of MPB NPs by number and volume.

S3: The zeta potential of MPB NPs

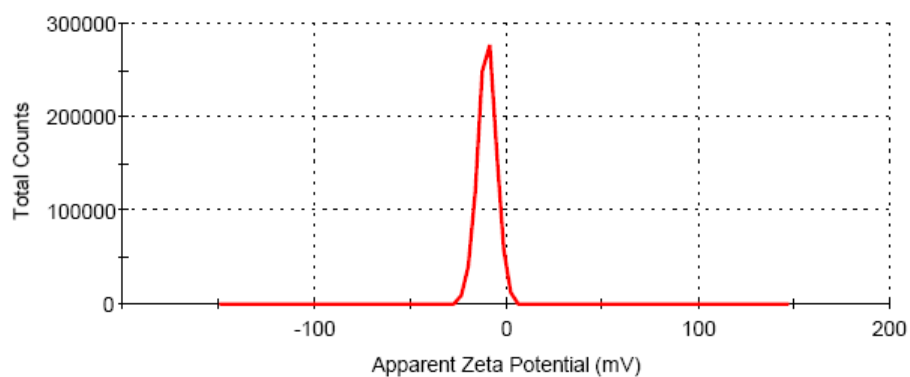


Figure S3. The zeta potential of MPB NPs (-10.1 mV).

S4: The size stability of MPB NPs

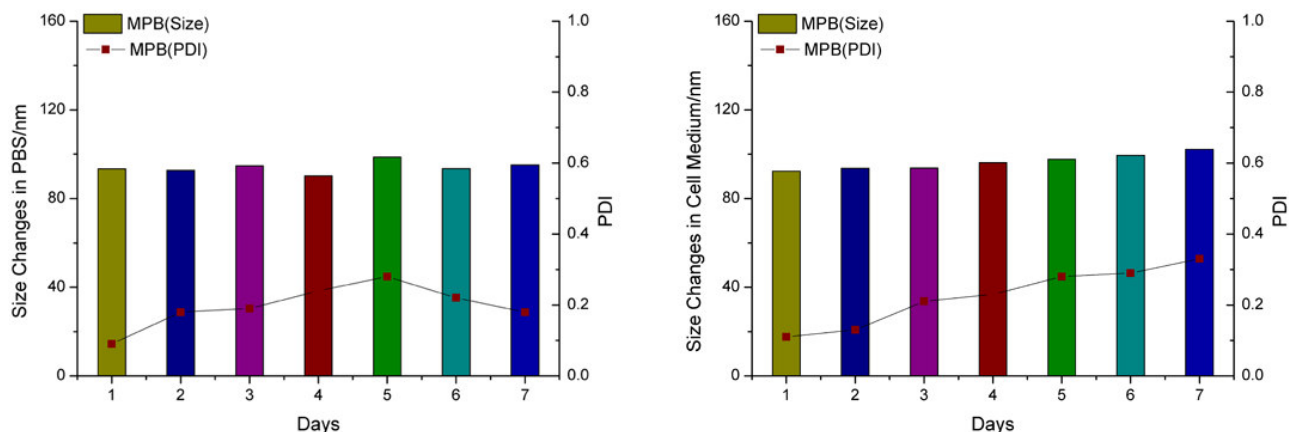


Figure S4. The size change of MPB NPs in PBS and cell medium.

S5: The particle size distribution of LMWHA-MPB NPs

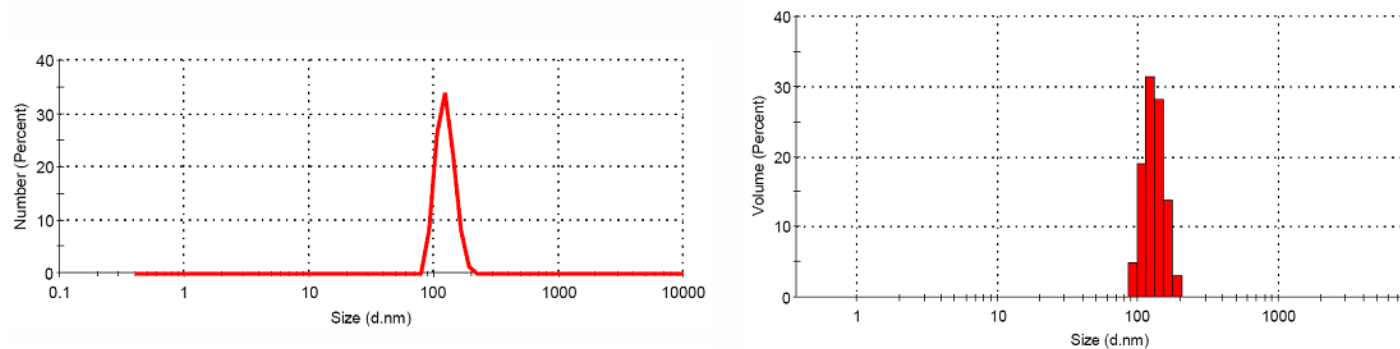


Figure S5. The DLS measurement results of LMWHA-MPB NPs by number and volume.

S6: The size stability of LMWHA-MPB NPs

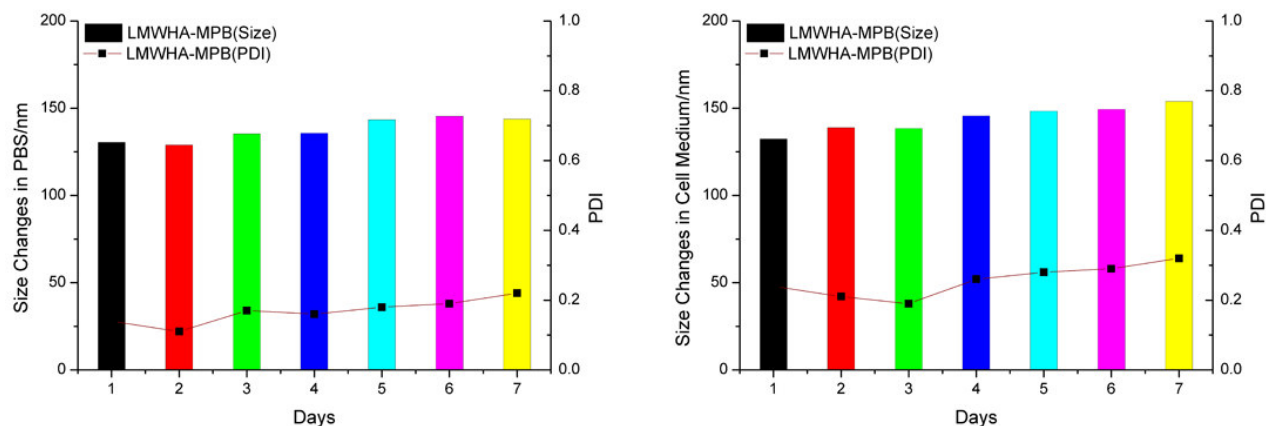


Figure S6. The size change of LMWHA-MPB NPs in PBS and cell medium.

S7: Characterization of LMWHA-MPB/HMME

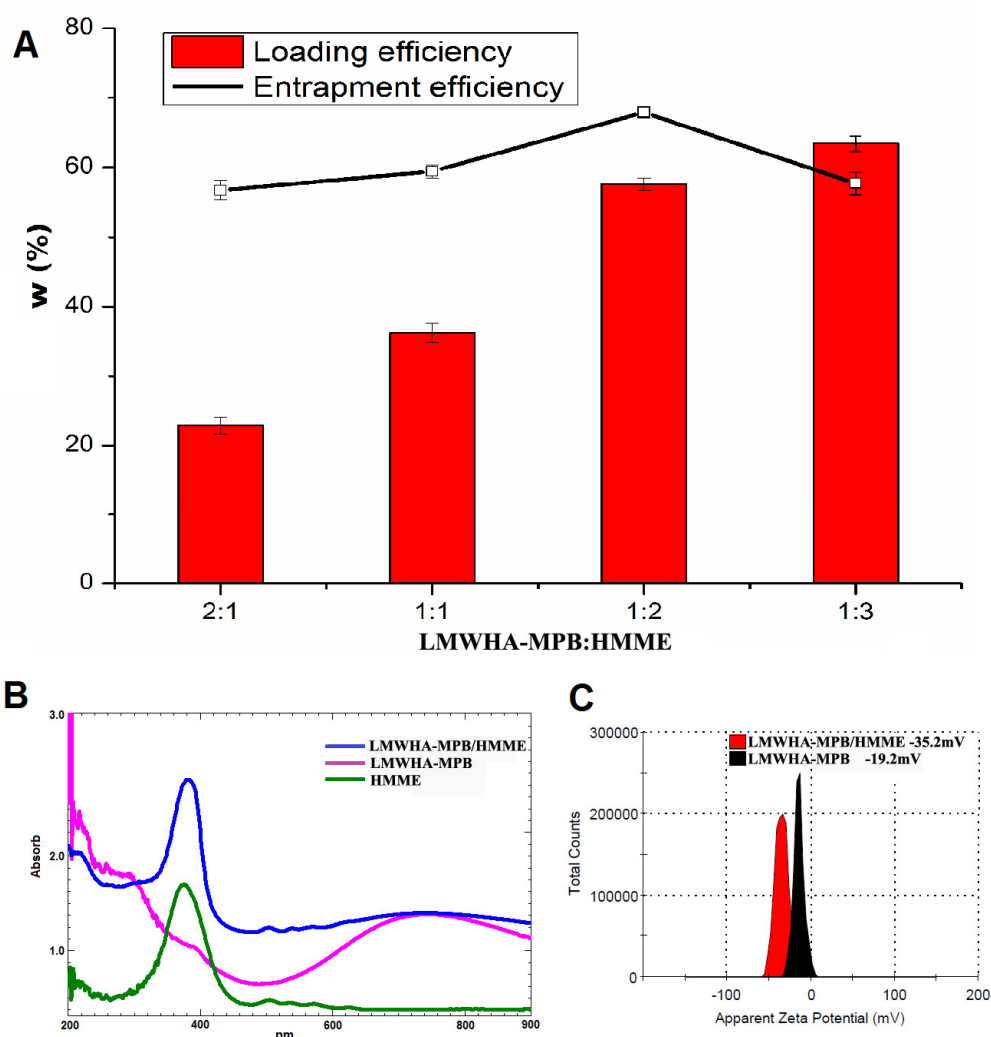


Figure S7. A: Loading efficiency and entrapment efficiency of HMME at different feeding LMWHA-MPB: HMME weight ratios; B: UV-vis spectrum of LMWHA-MPB/HMME, LMWHA-MPB and HMME; C: Apparent zeta potentials of LMWHA-MPB/HMME(-35.2 mV) and LMWHA-MPB (-19.2 mV).

S8. Internalization of FITC-labeled MPB and LMWHA-MPB NPs by M2 macrophages

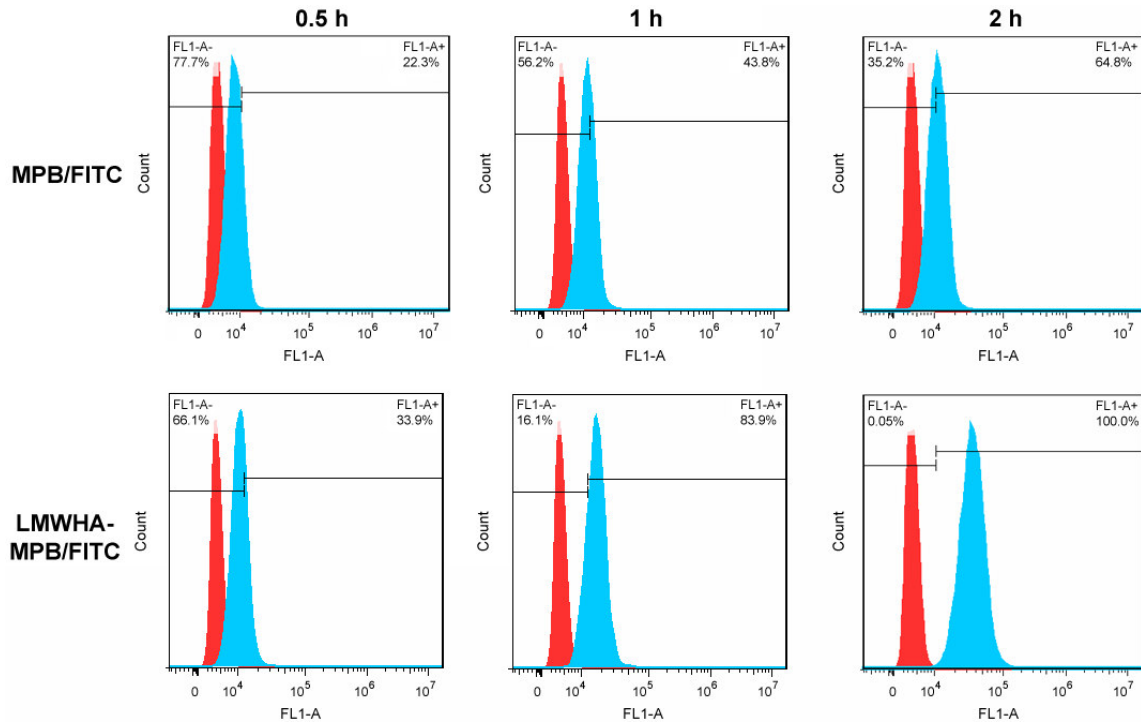


Figure S8. Internalization of FITC-labeled MPB and LMWHA-MPB NPs by M2 macrophages determined by flow cytometry

S9. The expression level of MMP-9 and VEGF determined by ELISA method

For cell migration and invasion experiment, the expression level of main correlated cytokines like matrix metalloprotein-9 (MMP-9) and vascular endothelial growth factor (VEGF) were determined after 4T1 and macrophages co-culture by enzyme-linked immunosorbent assay (ELISA). Briefly, 4T1 cells were seeded into 24-well plates at a density of 5×10^4 cells/well. After incubation for 24 h, cells were washed and treated with 600 μ L of serum-free medium, M2 conditioned medium, MPB pre-treated M2 conditioned medium and LMWHA-MPB pre-treated M2 conditioned medium, respectively. The intervention time was 24 h. After that, the cell culture mediums of each group were collected, and the supernatant solutions were transferred to sterile EP tubes for MMP-9 and VEGF determination using ELISA method after centrifugation (3500 rpm, 10 min).

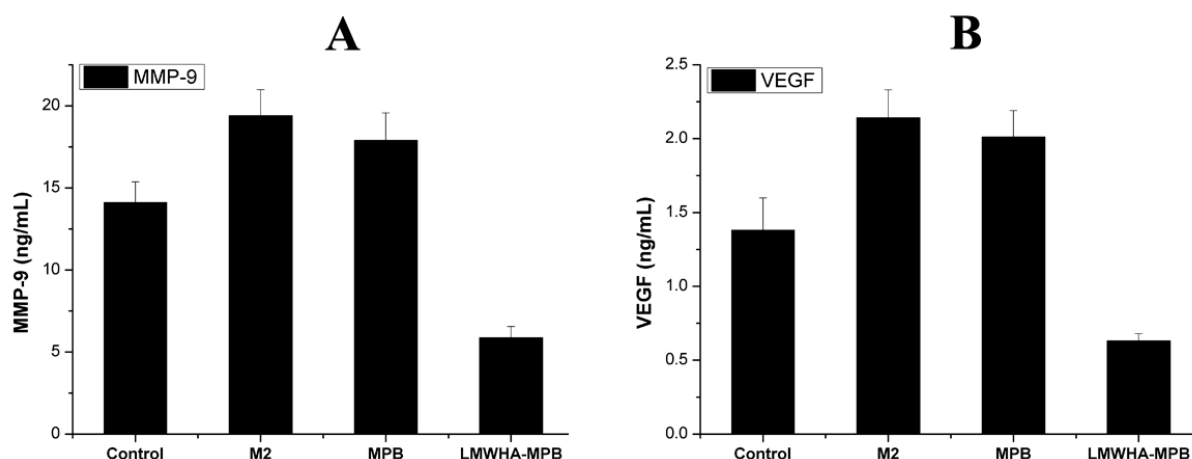


Figure S9. The expression level of MMP-9 and VEGF proteins after 4T1 cells treated with serum-free medium (Control group), M2 conditioned medium (M2 group), MPB pre-treated M2 conditioned medium (MPB group) and LMWHA-MPB pre-treated M2 conditioned medium (LMWHA-MPB group), respectively for 24 h.

S10. O₂ production in the reaction of MPB with H₂O₂

Add MPB or LMWHA-MPB NPs dispersion into H₂O₂ solution with the final concentration of MPB and H₂O₂ being 10 μg/mL and 2 mM, respectively. Take photographs to record O₂ production. Furthermore, in order to quantitatively determine and compare the catalytic activities of MPB and LMWHA-MPB NPs, the portable dissolved oxygen analyzer was used to quantitatively determine the O₂ concentration in the solution.

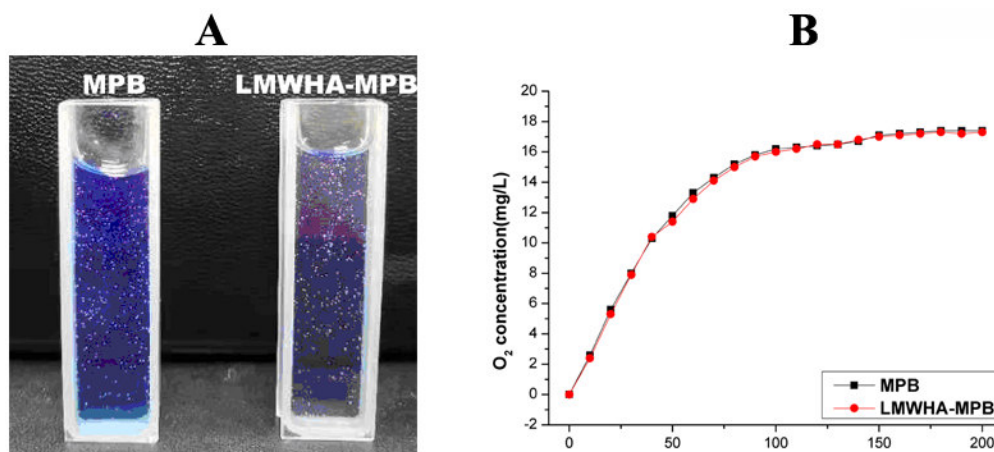


Figure S10. (A) The photograph of O₂ production after adding MPB or LMWHA-MPB NPs into H₂O₂ solution. (B) The changes of O₂ concentration in the solution determined by portable dissolved oxygen analyzer.

S11. Determination of H₂O₂ production in vitro

RAW264.7 cells pretreated with IL-4 were incubated with or without LMWHA-MPB (50 µg/mL) for 3h. After that, cells were washed with PBS and incubated for 24h. After trypsinization and centrifugation, cells were collected in PBS buffer and broken by an ultrasonic cell disruptor. Then the supernatant was collected to detect H₂O₂ level in the medium using H₂O₂ Assay Kit (A064-1). Meanwhile, RAW264.7 cells without IL-4 pretreatment were used as the control group.

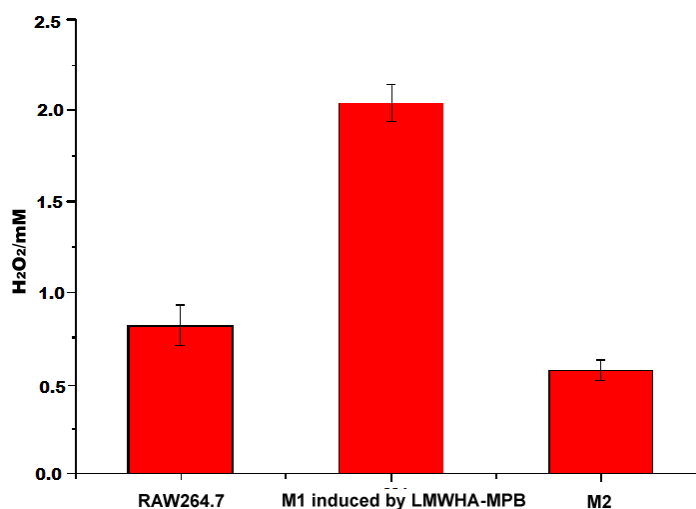


Figure S11. The quantitative determination of RAW264.7, M2 and M1-type macrophages producing H₂O₂ in vitro.

S12. The visual image of tumor tissues after the mice were sacrificed

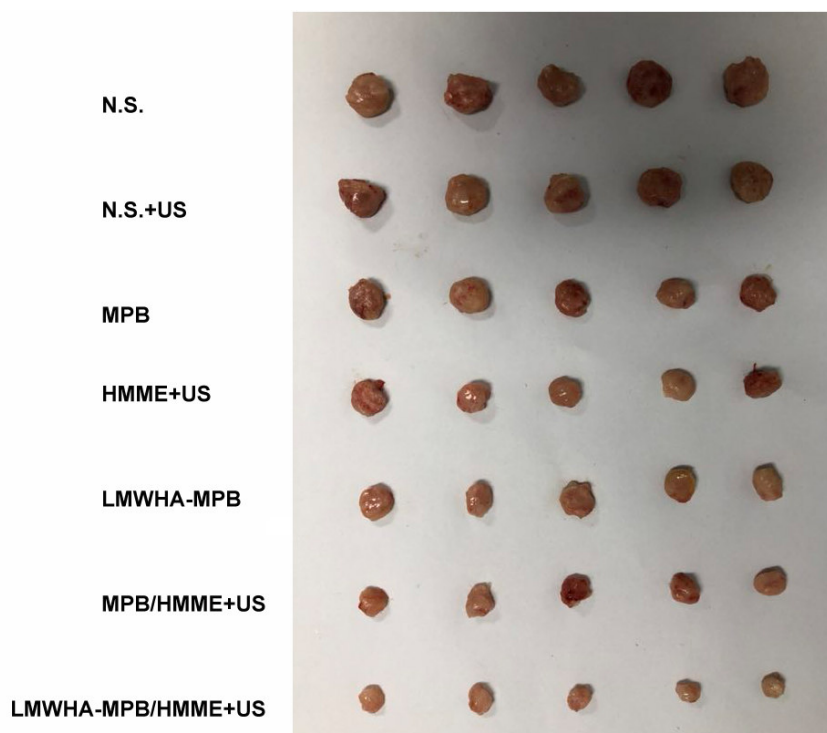


Figure S12. The visual image of tumor tissues after the mice were sacrificed.

S13. In vivo ROS detection.

Tumor-bearing mice were intravenously administered with (1) N.S.; (2) HMME; (3) MPB/HMME; (4) LMWHA-MPB/HMME, respectively (10 mg/kg). The tumor sites in above groups were exposed to US stimulation (3 MHz, 1.0 W/cm²) for 1.0 min at 2 h post-injection. After that, the mice were sacrificed and tumors were removed, followed by covering with cryo-embedding compound OCT and freezing at -80 °C until sectioning. Slices (15 μm) were prepared with frozen section machine. The sections were stained with DCFH-DA for analysis.

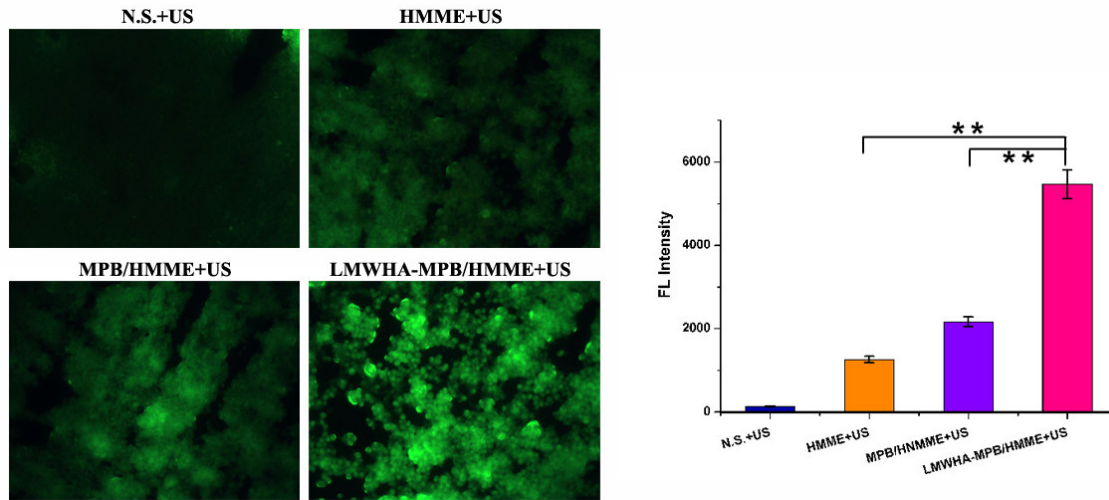


Figure S13. The ROS detection results and fluorescence intensity statistics of tumor frozen sections treated with various preparations combining with US. (*P < 0.05 and **P < 0.01)

S14. CD31 expression in tumor tissues

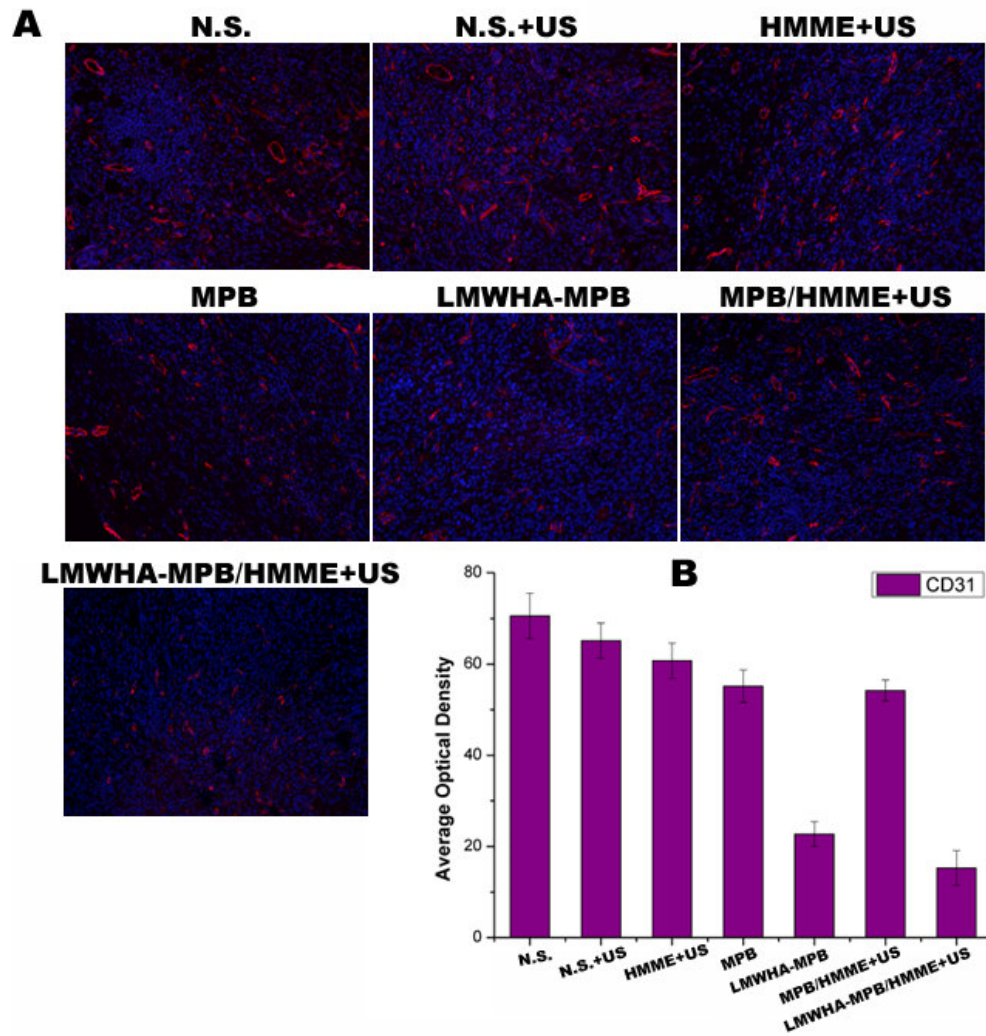


Figure S14. (A) Representative immunofluorescence images of tumor slices stained by CD31-PE. (B) The quantitative AOD values of vascular density (CD31, red) in histogram.

S15 and S16. The toxicity evaluation of the formulations

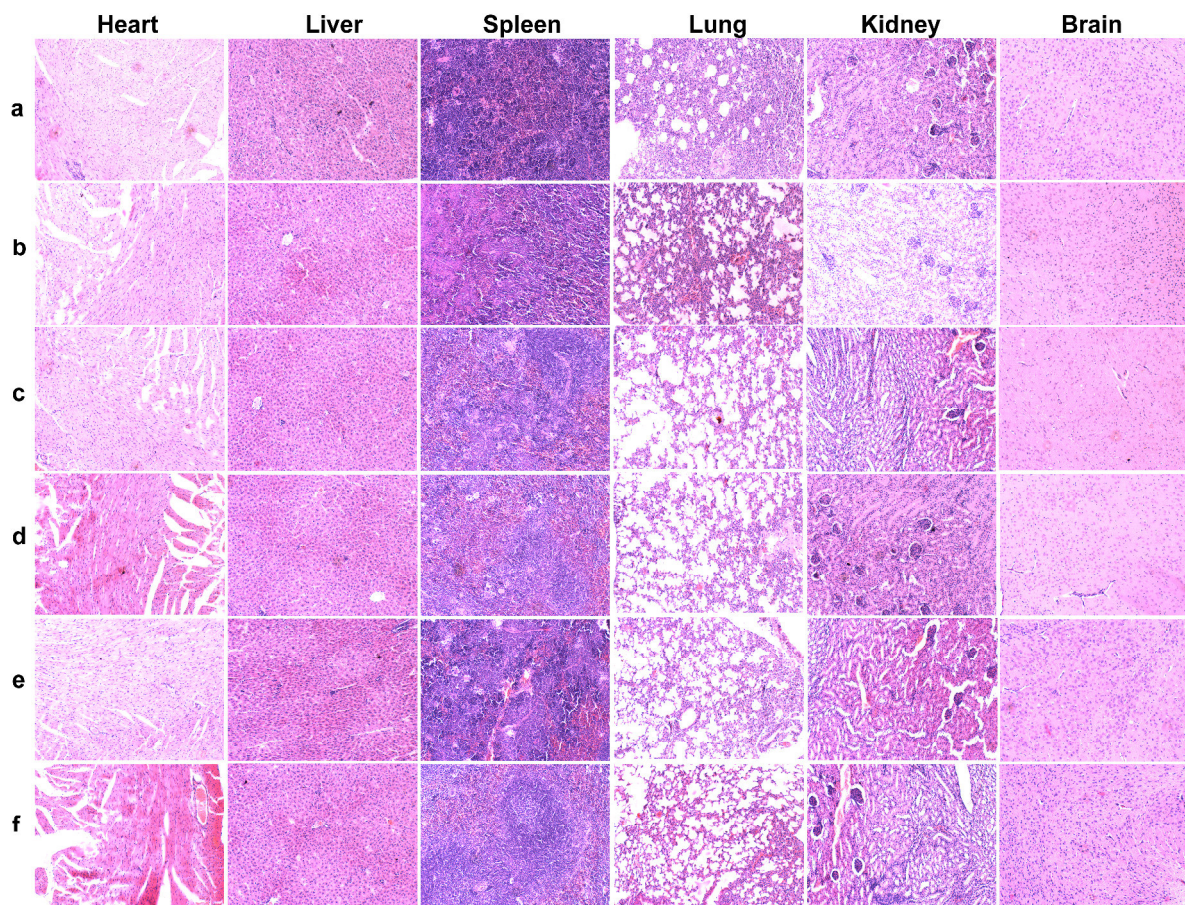


Figure S15. In vivo toxicity evaluation by histological examination. H&E stained tissues were harvested from the health mice which were treated with different formulations. (a) N.S., (b) MPB, (c) LMWHA-MPB, (d) HMME, (e) MPB/HMME, (f) LMWHA-MPB/HMME.

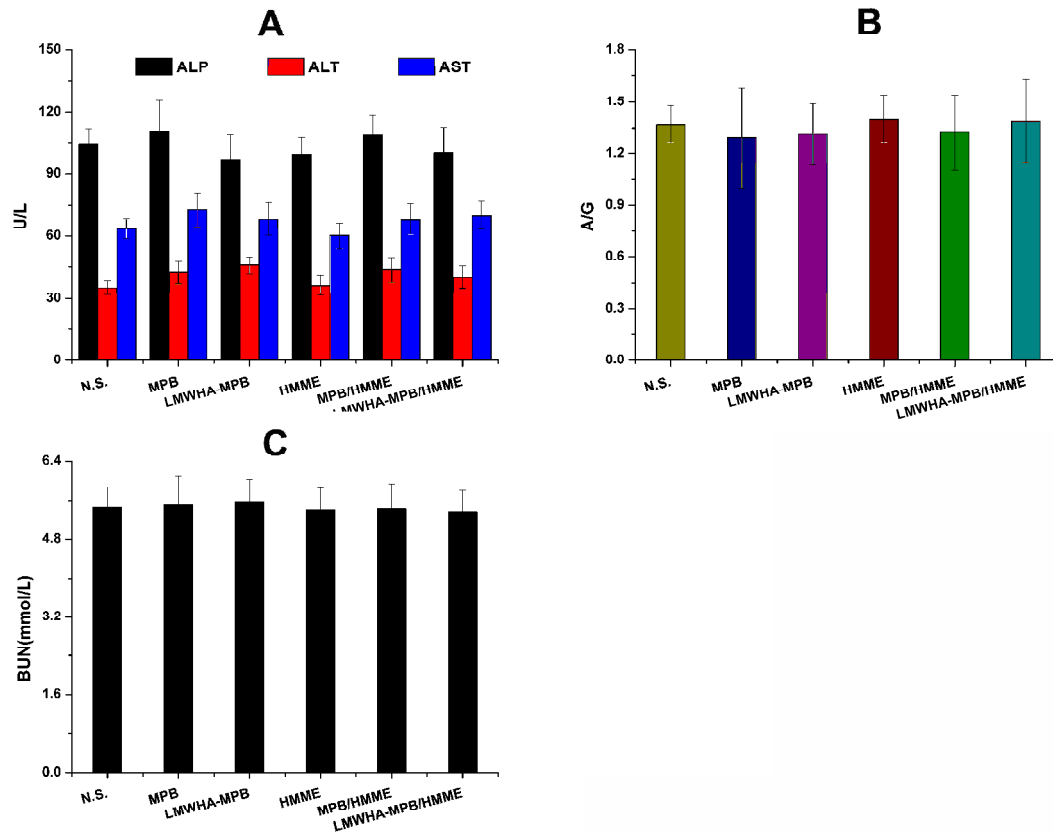


Figure S16. In vivo toxicity evaluation by the serum biochemistry assay. (A) Liver function markers including alanine aminotransferase (ALT), aspartate aminotransferase (AST) and alkaline phosphatase (ALP). (B) The index of liver function: albumin/globin (A/G) ratios. (C) The renal function indicator: blood urea nitrogen (BUN).